# High-Harmonic Fast-Wave Power Flow along Magnetic Field Lines in the Scrape-Off Layer of NSTX

R. J. Perkins,[1,*] J. C. Hosea,[1] G. J. Kramer,[1] J.-W. Ahn,[2] R. E. Bell,[1] A. Diallo,[1] S. Gerhardt,[1] T. K. Gray,[2] D. L. Green,[2] E. F. Jaeger,[3] M. A. Jaworski,[1] B. P. LeBlanc,[1] A. McLean,[2] R. Maingi,[2] C. K. Phillips,[1] L. Roquemore,[1] P. M. Ryan,[2] S. Sabbagh,[4] G. Taylor,[1] and J. R. Wilson[1]

[1]*Princeton Plasma Physics Laboratory, Princeton, New Jersey, USA*
[2]*Oak Ridge National Laboratory, Oak Ridge, Tennessee, USA*
[3]*XCEL Engineering Inc., Oak Ridge, Tennessee, USA*
[4]*Columbia University, New York, USA*

(Received 23 February 2012; published 27 July 2012)

A significant fraction of high-harmonic fast-wave (HHFW) power applied to NSTX can be lost to the scrape-off layer (SOL) and deposited in bright and hot spirals on the divertor rather than in the core plasma. We show that the HHFW power flows to these spirals along magnetic field lines passing through the SOL in front of the antenna, implying that the HHFW power couples across the entire width of the SOL rather than mostly at the antenna face. This result will help guide future efforts to understand and minimize these edge losses in order to maximize fast-wave heating and current drive.

DOI: 10.1103/PhysRevLett.109.045001 PACS numbers: 52.50.Qt, 52.35.−g, 52.55.Fa, 52.70.Gw

*Introduction.*—High-harmonic fast-wave (HHFW) heating and current drive are being explored on the National Spherical Torus Experiment (NSTX) to assist in plasma startup and to sustain $H$-mode plasmas. However, a significant fraction of the HHFW power can be lost at the edge of NSTX—up to 60% for current drive phasing—and part of this lost power can subsequently propagate to the divertor regions outside the outer strike radii [1,2]. This process is apparent in optical camera images (Fig. 1), where bright spirals form on both the upper and lower divertor regions during the application of rf power. This spiral delivers a large heat flux to the divertor, up to 2 $\mathrm{MW/m^2}$ when an rf power of 2 MW is applied as measured with IR cameras [2]. In addition, divertor tile currents [3] and Langmuir probes [4,5] show strong responses to the rf pulse when these diagnostics lie underneath the spiral. The mechanism behind this loss of rf power in the scrape-off layer (SOL) must be understood and minimized to realize the full potential of HHFW heating and current drive both in NSTX and in conventional fast-wave heating regimes in general. This is an important consideration for ITER for preventing excessive erosion on the divertor floor for the planned 20 MW of long-pulse fast-wave heating.

We show here that field-line mapping from the SOL midplane in front of the antenna to the divertor elucidates many experimental observations of the rf spiral. In particular, we conclude that much of the spiral is not magnetically connected to the antenna screen or limiters but rather to the SOL in front of the antenna. In this regard, this edge loss of rf power resembles divertor erosion studies on $C$-Mod [6] and differs considerably from the well-studied loss of rf power directly to the fast-wave antenna [7,8] that can result in substantial erosion and impurity generation [9,10]. Much effort has been directed to minimize erosion through proper antenna design [11], but the present work suggests that the primary loss of rf power on NSTX occurs along the open field lines in the SOL, not at the antenna, and may require different remediation. Importantly, all of the losses in the outboard SOL must be minimized to maximize the fraction of fast-wave power that enters the core plasma.

This Letter will first present various effects of the rf spiral and the changes in these effects as the magnetic pitch in NSTX is altered. Field-line mapping will then be used to explain these observations, leading to the conclusion that the rf power flows through the SOL to the divertor mostly along field lines that originate not on the antenna but throughout the SOL in front of the antenna. We conclude by hypothesizing that the underlying mechanism for this loss of power is fast-wave propagation in the SOL and that this effect is likely to be present to some degree for fast wave heating generally. Note that the slow wave is strongly cutoff in front of the antenna.

*Experimental properties of the rf spiral.*—The rf spiral moves radially across the divertor floor (ceiling) as the magnetic field pitch in NSTX is varied, suggesting that the flow of rf power reaching the divertor region through the SOL is closely aligned along field lines. In Fig. 1, the major radius of the spiral decreases by up to 15 cm at any given toroidal location as a result of increasing the pitch between shots. The images in Fig. 1 are in the optical domain, and the pitch is increased from $\sim 31°$ at the antenna to $\sim 40°$ by adjusting the plasma current (poloidal magnetic field) and the toroidal magnetic field. The ability to control the spiral position means that the spiral can be moved onto and off of diagnostics in the divertor to determine the effects of the rf power deposition on the diagnostic signals.

For instance, the currents to certain divertor tiles [3] can respond sharply to the onset of rf power depending on

 

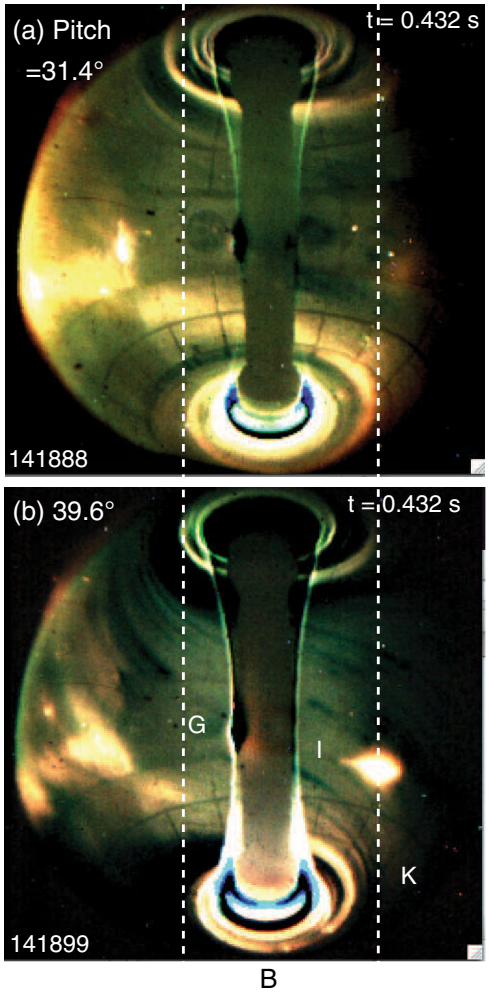


FIG. 1 (color online). The edge rf power deposition moves radially inward as the magnetic field pitch increases. (a) A pitch of 31° in front of the antenna, given by $B_T = 5.5$ kG, $I_P = 0.8$ MA; (b) 40° for $B_T = 4.5$ kG, $I_P = 1.0$ MA. Contrast enhanced with subtraction of background at $t = 0.247$ s (before rf pulse). Antenna is on the left and Bay $B$, $G$, $I$, and $K$ locations are indicated. The bright blob on the right of (b) is due to gas injection.

the magnetic pitch. Figure 2(a) shows the tile-current responses over the course of a magnetic-pitch scan that covers a pitch range of ~31° to ~40° in front of the antenna. For these shots, the rf power ($P_{rf}$) is 1.4 MW in a deuterium $H$-mode plasma produced with a neutral beam power ($P_{NB}$) of 2 MW. The extremes of this scan are the conditions for the spiral pictures of Fig. 1. Currents are shown for tiles 3g, 3i, and 3k, located at major radii 0.853 m $< R <$ 0.946 m at Bays G, I, and K noted in Fig. 1(b). Tile 3g lies outside the spiral zone, and its current is not affected by the rf pulse. Tiles 3i and 3k, however, clearly respond to the rf pulse, but the strength of this response depends on the magnetic field pitch. Figure 2(b) plots the average amplitude of these responses as a function of field pitch; as the spiral moves radially inward, it moves off of tile 3k and fully onto tile 3i. The rf-induced current corresponds to an electron current to the tile, which is consistent with enhanced electron losses due to an local rf field and also with rf heating of the plasma along the magnetic field lines leading to the spiral.

Likewise, Langmuir-probe [4,5] data track the spiral movement across the divertor floor. At the highest pitch of ~40° the spiral is pushed partly over a four-probe array located at 0.638 m $< R <$ 0.706 m at Bay $B$ (see Fig. 1). The outermost probe, probe 4, intercepts the spiral, and its floating potential ($V_f$) is pushed to negative values during the rf pulse as shown in Fig. 3 (note that the rf arcs strongly modulate $V_f$). Meanwhile, probe 2, just 6 cm inboard of probe 4, is little affected, showing that the rf effect on the probes is localized to the spiral. Moreover, the negative shift in floating potential is consistent with both the effect expected from the presence of an rf field and heating of the plasma in the spiral.

*Magnetic field line mapping.*—Field-line mapping from the SOL midplane to the divertor explains the experimental observations noted above: the spiralled geometry of the rf power deposition on the divertor, the movement of the spiral as pitch is changed, and the diagnostic response to the applied

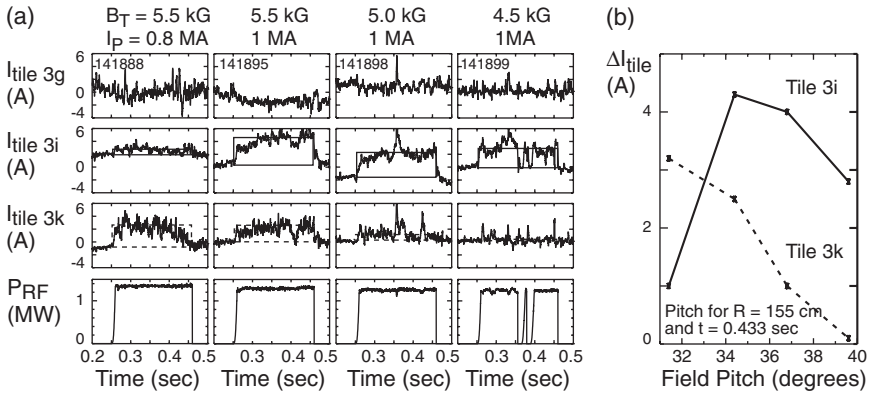


FIG. 2. (a) Row 3 divertor tile currents at Bays $G$, $I$, and $K$ versus time for four ratios of $I_p/B_T$. (b) Tile 3i and 3k currents versus field pitch in front of the antenna. $k_\parallel = -9$ m$^{-1}$, $\phi_{Ant} = -90°$, $D_2$, $P_{NB} = 2$ MW.

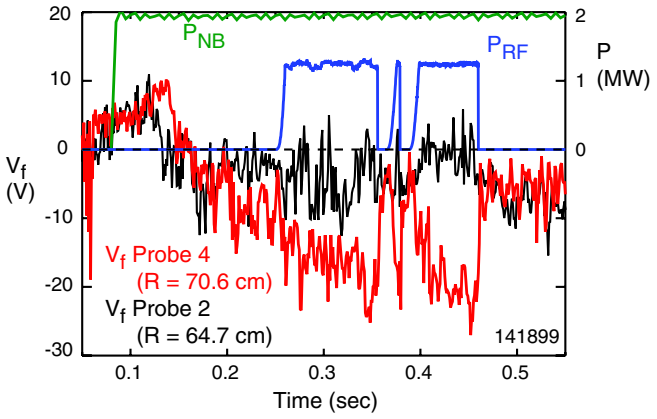


FIG. 3 (color online). Probe 4 of the Langmuir-probe array responds to rf at the highest pitch when the spiral moves over it. Probe 2, 6 cm inboard and not under the spiral, shows almost no response to the rf. The pitch at the antenna is 39.6° here.

rf. The field lines are computed using the full-orbit code SPIRAL [12], which follows the motion of charged particles. The particle orbits can be taken as proxies for the magnetic field lines if the particle energies are small (1 eV deuterons here) and if the particles are launched parallel to the field to minimize grad-$B$ drifts. SPIRAL uses EFIT [13] equilibrium magnetic field reconstructions for NSTX discharges.

The field-line mappings reproduce the rf spiral when field lines from across the SOL midplane in front of the antenna are included. Figure 4 plots three sets of field lines originating in the SOL midplane in front of the antenna at selected major radius values ($R_{SOL}$) of 1.55 m, 1.53 m and 1.52 m; the field lines are then followed until they strike the lower divertor. These $R_{SOL}$ values lie between the antenna radius of 1.575 m and the last closed flux surface (LCFS) radius of 1.515 m. The field lines generate a spiral pattern similar to the visible camera images in Fig. 1. Although the antenna spans 90° toroidally, the lines converge radially as they wind around the center column, and lines starting closer to the LCFS strike the divertor farther in radially and wrap around the center column more toroidally. Only field lines in the SOL that start well away from the antenna wrap around enough to match the spirals seen in camera images and reach the Langmuir probe array described above. Thus, the spiral is caused by rf power flowing mostly along field lines originating across the SOL midplane between the LCFS and the antenna face as opposed to originating solely from the antenna face.

Field-line mapping also reproduces the movement of the rf spiral as the magnetic pitch is altered. Figure 5 plots the points at which the field lines strike the lower divertor or vessel region; all the field lines that pass in front of the antenna at the midplane are included (omitting lines passing in front of the lower left and upper right antenna corners which exhibited little interaction with the edge plasma), and equilibrium reconstructions for the two pitch cases of Fig. 1 are used. Field lines are started at midplane radii from 157.5 cm to 152 cm in increments of 0.25 cm; the particles

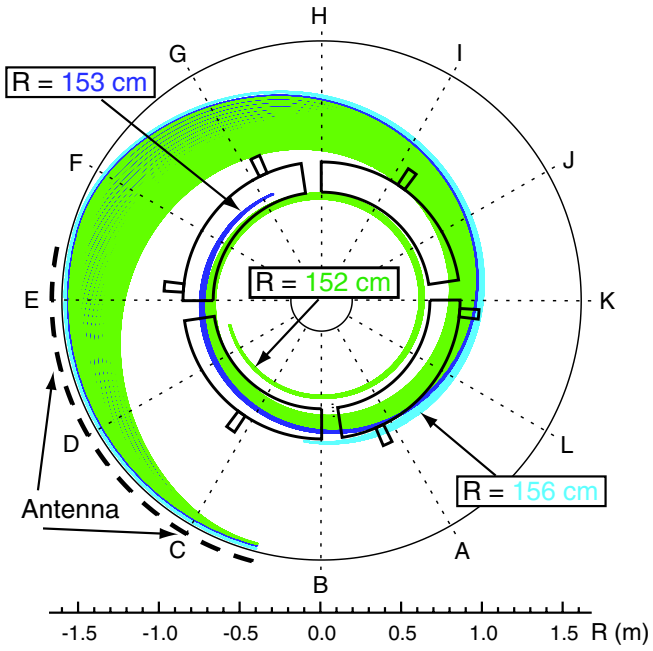


FIG. 4 (color online). Three sets of field lines originating in the SOL midplane in front of the antenna are plotted for midplane radii of 1.55 (light blue), 1.53 (dark blue), and 1.52 m (green). The field lines are integrated until they terminate on the lower divertor region. View from above. Note that field lines starting at smaller radii wrap around the center post more and terminate further in radially.

are color-coded to denote their starting radius. The entire set of strike points defines a spiral and reveals that the high-pitch spiral [Fig. 5(b)] is rotated counter-clockwise relative to the low-pitch spiral [Fig. 5(a)] because the larger downward field component causes the field lines to not travel as far toroidally before striking the divertor. The movement of the computed strike points with pitch agrees with the actual movement of the spiral on the lower divertor floor shown in Fig. 1.

Figure 5 also explains the response of the tile currents and Langmuir probes to the application of rf power as a function of magnetic pitch. It shows that the strike-point spiral moves off tile 3k and onto tile 3i with the increase in magnetic pitch in close agreement with the data of Fig. 2. In addition, the locations of the spiral at Bay $B$, where the radial Langmuir probe array sits, explain the response of the observed Langmuir probe signals. The strike-point spiral misses Probe 4, the outermost probe, at the lower pitch but moves over Probe 4 at the higher pitch. Probe 4 shows a response to the rf only on the highest-pitch shot (Fig. 3), indicating that this is the only shot for which the spiral has moved far enough inward at Bay $B$ to reach the probe array. The agreement between the field-line computations and the experimental measurements suggest that the rf effects are confined to field lines from the SOL midplane in front of the antenna and only influence diagnostics when those field lines intercept the diagnostics.

*Conclusion.*—Fast-wave heating and current drive can be hindered on NSTX when a significant loss of the fast wave

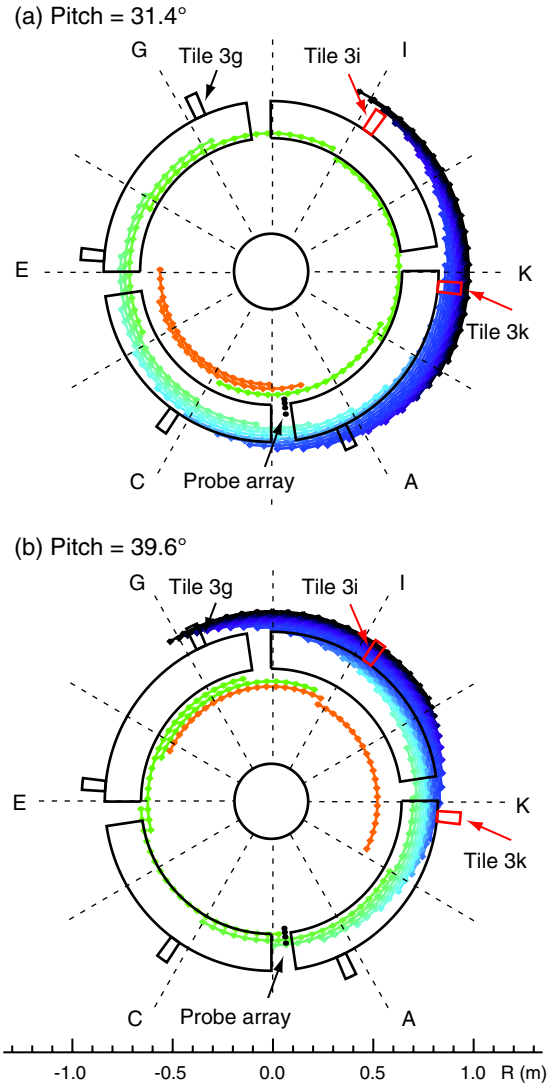


FIG. 5 (color online). Locations of the field strike points on the bottom divertor vs field pitch with the midplane SOL radius varying between 157 and 152 cm (antenna radius = 157.5 and LCFS radius = 151.5 cm). The movement of the spiral over the instrumented divertor tiles and Langmuir-probe array is apparent.

power to the SOL and divertor region occurs. This loss of fast wave power does not occur solely at the antenna Faraday screen and limiters but rather across the SOL in front of the antenna. The lost rf power, whether carried through the SOL by wave propagation and/or by rf-driven particle flux, then flows primarily along magnetic field lines and is ultimately deposited on the divertor, giving rise to the bright spirals and modifying signals from diagnostics such as the Langmuir probes and instrumented divertor tiles. These conclusions are reached by the close agreement between experimental observations and the magnetic field line mappings.

The underlying mechanism behind this edge loss has not yet been identified, but we hypothesize that fast waves are excited in the SOL and propagate to the divertor. Previous experiments demonstrated that core power deposition is a strong function of both the parallel wavelength and magnetic field close to the antenna in keeping with the functional dependence of the onset density for perpendicular fast-wave propagation ($n_{\mathrm{onset}} \approx Bk^2/q\mu_0\omega$ from cold plasma theory) [14,15]. In fact, the edge rf power deposition decreases substantially when the onset density is pushed a few centimeters away from the antenna [1,2,14–16]. The location at which the plasma density exceeds the onset density for perpendicular wave propagation typically occurs a few centimeters away from the antenna, a location apparently consistent with the field-line mapping. Alternatively, the edge loss to the divertor might involve other mechanisms: heating of SOL particles, dc currents produced by rf reactive and propagating fields at the antenna, and enhanced sheath dissipation due rf rectification. The results presented here stress the need for SOL measurements to locate wave propagation. Also, advanced code simulations of the rf edge power deposition in the SOL (e.g., [17]) should find rf power flow to the divertor region primarily aligned with the magnetic field lines. These steps are certainly needed to understand and minimize such edge losses in the ion cyclotron range of frequencies heating regime and could be important for ITER.

This work was supported by DOE Contract No. DE-AC02-09CH11466. The authors would like to thank Doctor M. Ono and Doctor J. Menard for their continued support.

*rperkins@pppl.gov

[1] J. C. Hosea *et al.*, AIP Conf. Proc. **1187**, 105 (2009).
[2] G. Taylor *et al.*, Phys. Plasmas **17**, 056114 (2010).
[3] S. P. Gerhardt, E. Fredrickson, L. Guttadora, R. Kaita, H. Kugel, J. Menard, and H. Takahashi, Rev. Sci. Instrum. **82**, 103502 (2011).
[4] M. A. Jaworski, J. Kallman, R. Kaita, H. Kugel, B. LeBlanc, R. Marsala, and D. N. Ruzic, Rev. Sci. Instrum. **81**, 10E130 (2010).
[5] J. Kallman, M. A. Jaworski, R. Kaita, H. Kugel, and T. K. Gray, Rev. Sci. Instrum. **81**, 10E117 (2010).
[6] S. J. Wukitch *et al.*, AIP Conf. Proc. **933**, 75 (2007).
[7] P. Jacquet *et al.*, Nucl. Fusion **51**, 103018 (2011).
[8] L. Colas *et al.*, AIP Conf. Proc. **787**, 150 (2005).
[9] J. E. Stevens *et al.*, Plasma Phys. Controlled Fusion **32**, 189 (1990).
[10] M. Bures, J. Jacquinot, K. Lawson, M. Stamp, H. P. Summers, D. A. D'Ippolito, and J. R. Myra, Plasma Phys. Controlled Fusion **33**, 937 (1991).
[11] V. Bobkov *et al.*, AIP Conf. Proc. **1187**, 125 (2009).
[12] G. J. Kramer *et al.*, in Proceedings of the 22nd International Fusion Energy Conference, Geneva, 2008, http://www-pub.iaea.org/MTCD/Meetings/FEC2008/it_p6-3.pdf.
[13] S. A. Sabbagh *et al.*, Nucl. Fusion **41**, 1601 (2001).
[14] J. Hosea *et al.*, Phys. Plasmas **15**, 056104 (2008).
[15] C. K. Phillips *et al.*, Nucl. Fusion **49**, 075015 (2009).
[16] J. C. Hosea *et al.*, AIP Conf. Proc. **1406**, 333 (2011).
[17] D. L. Green, L. A. Berry, G. Chen, P. M. Ryan, J. M. Canik , and E. F. Jaeger , Phys. Rev. Lett. **107**, 145001 (2011).